

Mathematical Modelling and Analysis of Malaria Transmission Dynamics with Early and Late Treatment Interventions

Original Research
Article

Received: XX December 20yy

Accepted: XX December 20yy

Online Ready: XX December 20yy

Abstract

Malaria, a life-threatening disease caused by *Plasmodium* parasites transmitted through the bites of infected *Anopheles* mosquitoes, poses a persistent public health challenge in Nigeria due to its complex transmission dynamics. This study develops a compartmental SEIR-SEI model to evaluate the impact of early (λ_1) and late (λ_2) treatment interventions on malaria transmission among children under 5, aiming to guide effective control strategies. Parameterized with Nigerian malaria case data (2007–2021), the model integrates human and mosquito populations to examine how treatment timing affects the basic reproduction number (R_0) and disease prevalence. Using stability analysis, sensitivity analysis, and numerical simulations, we find a baseline $R_0 = 2.24$, indicating endemicity. Early treatment reduces this to $R_{0,\lambda_1} = 1.46$, outperforming late treatment ($R_{0,\lambda_2} = 1.65$). Sensitivity analysis highlights mosquito biting rates (b) and λ_1 as key drivers of R_0 . Simulations show that 60–80% early treatment coverage ($\lambda_1 \geq 0.6$) within 24 hours significantly lowers prevalence within 120 days, unlike 100% late treatment ($\lambda_2 = 1.0$). The disease-free equilibrium is stable when $R_0 < 1$, achievable with high λ_1 . Rapid diagnosis, Artemisinin-based Combination Therapies, and vector control are critical for eradication. Policymakers should enhance healthcare access and surveillance to reduce Nigeria's malaria burden.

Keywords: Malaria Transmission; Mathematical Modeling; Treatment Interventions; Basic Reproduction Number; Stability Analysis; Public Health

2010 Mathematics Subject Classification: 92B05; 92C60

1 Introduction

Malaria, transmitted by *Anopheles* mosquitoes, persists as a formidable public health challenge in Nigeria, where rapid disease spread and limited healthcare access amplify its toll (Bellomo, Li, & Maini, 2008). Mathematical modeling provides a robust framework to unravel the complexities of malaria transmission, enabling predictions of disease dynamics and evaluation of control measures (Li, 2014). This study develops a compartmental model to examine how the timing of treatment interventions influences malaria's spread, focusing on the interplay between human and mosquito populations. By incorporating early and late treatment effects, the model captures their impact on the basic reproduction number (R_0), disease prevalence, and equilibrium stability, offering insights

into optimizing treatment strategies. The research aims to guide public health policies in Nigeria, prioritizing timely interventions to curb malaria's burden and enhance resource allocation in endemic regions (Challenger et al., 2019).

2 Literature Review

Mathematical modeling is vital for understanding malaria transmission in high-burden regions like Nigeria, where *Plasmodium falciparum* drives significant morbidity (Mousa et al., 2020). Challenger et al. (2019) modeled treatment delays, finding that late treatment extends infectious periods, increasing transmission. Mousa et al. (2020) showed that delays beyond 24 hours raise severe malaria risk by 43% in children. Yunus and Olayiwola (2024) used fractional-order models to highlight early treatment's role in reducing R_0 , while Haile, Koya, and Mosisa Legesse (2024) emphasized early intervention for $R_0 < 1$. Anjorin et al. (2023) noted that presumptive treatment delays care, increasing transmission. This study addresses gaps by quantifying early versus late treatment effects using Nigerian data (2007–2021), establishing that 60–80% early treatment coverage rapidly reduces malaria prevalence (Challenger et al., 2019; Mousa et al., 2020).

3 Methodology

This study develops an eight-compartment SEIIR-SEI model to evaluate the effects of early and late treatment on malaria transmission, using ordinary differential equations (ODEs) parameterized with Nigerian malaria case data (2007–2021). The methodology encompasses model formulation, assumptions, parameter estimation, analytical methods, and numerical simulations.

3.1 Model Formulation

The model divides the human population ($N_h = S_h + E_h + I_{Eh} + I_{Lh} + R_h$) into Susceptible (S_h), Exposed (E_h), Infected with Early Treatment (I_{Eh}), Infected with Late Treatment (I_{Lh}), and Recovered (R_h). The mosquito population ($N_m = S_m + E_m + I_m$) includes Susceptible (S_m), Exposed (E_m), and Infectious (I_m). The system of ODEs, illustrated in Figure 1, is:

$$\frac{dS_h}{dt} = \alpha_h N_h - \sigma b \psi S_h I_m + \delta_3 R_h - \mu_h S_h, \quad (3.1)$$

$$\frac{dE_h}{dt} = \sigma b \psi S_h I_m - (\mu_h + \delta_1 + \delta_2) E_h, \quad (3.2)$$

$$\frac{dI_{Eh}}{dt} = \delta_1 E_h - (\mu_h + \eta_h + \lambda_1 + a) I_{Eh}, \quad (3.3)$$

$$\frac{dI_{Lh}}{dt} = \delta_2 E_h + a I_{Eh} - (\mu_h + \eta_h + \lambda_2) I_{Lh}, \quad (3.4)$$

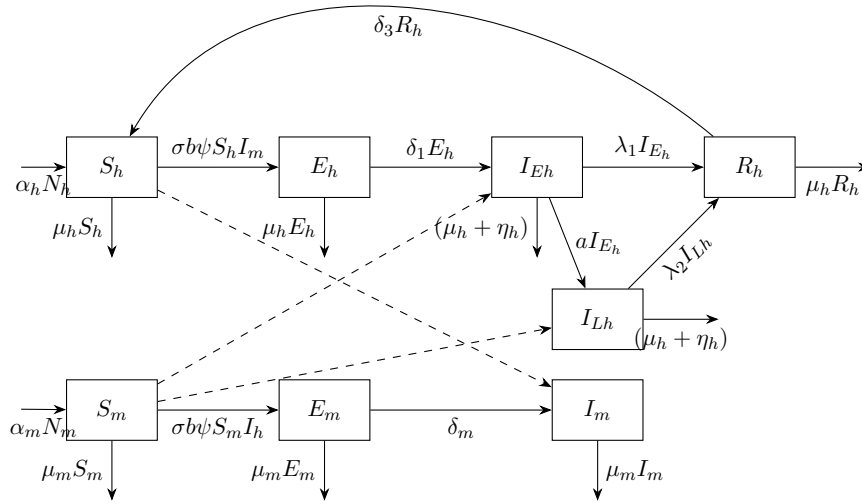
$$\frac{dR_h}{dt} = \lambda_1 I_{Eh} + \lambda_2 I_{Lh} - (\mu_h + \eta_h + \delta_3) R_h, \quad (3.5)$$

$$\frac{dS_m}{dt} = \alpha_m N_m - \sigma b (\psi I_{Eh} + \psi_1 I_{Lh}) S_m - \mu_m S_m, \quad (3.6)$$

$$\frac{dE_m}{dt} = \sigma b (\psi I_{Eh} + \psi_1 I_{Lh}) S_m - (\mu_m + \delta_m + \gamma_m) E_m, \quad (3.7)$$

$$\frac{dI_m}{dt} = \delta_m E_m - \mu_m I_m. \quad (3.8)$$

Figure 1: Flowchart for malaria transmission dynamics.



3.2 Assumptions

The model is based on the following assumptions:

1. Homogeneous mixing between human and mosquito populations.
2. Newborns are susceptible, and recovered individuals lose immunity over time (Mousa et al., 2020).
3. Early treatment (λ_1) is more effective than late treatment (λ_2) (Challenger et al., 2019).
4. Mosquito recruitment and mortality rates are constant.
5. Treatment protocols follow WHO recommendations (Anjorin et al., 2023).

3.3 Parameters and Variables

Parameters and variables are defined in Tables 1 and 2. Initial conditions are set based on Nigerian malaria prevalence data, assuming a 10:1 mosquito-to-human ratio.

Table 1: Model Parameters

Parameter	Description
μ_h, μ_m	Natural mortality rate (humans, mosquitoes)
α_h, α_m	Recruitment rate (humans, mosquitoes)
b	Probability of human infection per bite
c	Probability of mosquito infection per bite
σ	Mosquito biting frequency
ψ, ψ_1	Contact rates (early, late treatment infections)
δ_1, δ_2	Progression rates to early/late treatment
λ_1, λ_2	Recovery rates (early, late treatment)
η_h	Malaria-induced mortality rate (humans)
a	Rate of treatment loss (early to late)
δ_3	Rate of immunity loss
δ_m	Progression rate to infectious mosquitoes
γ_m	Mosquito exposed compartment loss rate

Table 2: Model Variables

Variable	Description
N_h, N_m	Total human and mosquito populations
S_h, E_h	Susceptible and exposed humans
I_{Eh}, I_{Lh}	Infectious humans (early, late treatment)
R_h	Recovered humans
S_m, E_m, I_m	Susceptible, exposed, and infectious mosquitoes

3.4 Parameter Estimation

Parameters are estimated using nonlinear least-squares fitting with malaria case data for children under 5 in Nigeria (2007–2021) (National Bureau of Statistics & United Nations Children's Fund, 2007, 2017; National Population Commission, 2018; United Nations Children's Fund, 2011, 2021). Some parameters are sourced from literature (Ducrot, Sirima, Somé, & Zongo, 2009; Kbenesh, 2009; World Health Organization, 2019). The data for S_m , E_m , and I_m were calculated based on a 10:1 mosquito-to-human ratio and exposure of 5% and 10%, respectively. The total human population for each year was derived from summing all human population categories (Table 3).

Year	S_h (Susceptible)	E_h (Exposed)	I_{Eh} (Infected, Early)	I_{Lh} (Infected, Late)	R_h (Recovered)	S_m (Susceptible)	E_m (Exposed)	I_m (Infected)
2007	16486	603.9	1264.6	1172.7	2431	164860	8243	824
2011	23730	676.9	204.4	878.0	2207	237300	11865	1186
2016/2017	176412	2630	147.95	1700.93	1479.10	1764120	88206	8821
2018	28094	7105	1381.59	2398.38	2619.70	280940	14047	1405
2021	10806	3226	1310.53	2132.29	3208.34	108060	5403	540

Table 3: Estimated population sizes for human and mosquito compartments in malaria transmission dynamics from 2007 to 2021.

3.5 Analytical Methods

The basic reproduction number (R_0) is computed using the next-generation matrix method (Van den Driessche & Watmough, 2002). Stability of the disease-free equilibrium is analyzed using the Jacobian matrix and Routh-Hurwitz criteria (Castillo-Chavez & Song, 2004). Global stability is assessed using the Castillo-Chavez approach. The normalized forward sensitivity index is defined as:

$$\xi_p^{R_0} = \frac{\partial R_0}{\partial p} \times \frac{p}{R_0}. \quad (3.9)$$

3.6 Numerical Simulations

The ODE system (Equations 3.1–3.8) is solved using the fourth-order Runge-Kutta method in Python. Sensitivity indices (Equation 3.9) are computed to identify parameters most influencing R_0 . Simulations explore the effects of varying recovery rates (λ_1, λ_2) and malaria-induced mortality (η_h).

The model provides a framework to assess treatment timing effects, with results presented in Section 4.

4 Main Result

This section presents the core mathematical and numerical results of the malaria transmission model, including the basic reproduction number (R_0), positivity and boundedness of solutions, stability of the disease-free equilibrium (DFE), existence of the endemic equilibrium (EE), parameter estimation, sensitivity analysis, and numerical simulations.

4.1 Basic Reproduction Number (R_0)

The basic reproduction number R_0 represents the average number of secondary infections caused by a single infected individual in a fully susceptible population. Using the next-generation matrix method (Van den Driessche & Watmough, 2002), as outlined in Section 3.5, R_0 is derived as:

$$R_0 = \frac{b\sigma\sqrt{\alpha_h\alpha_m\delta_m[a(\delta_1\psi + \delta_2\psi_1) + (\delta_1\psi(\eta_h + \lambda_2 + \mu_h) + \delta_2\psi_1(\eta_h + \lambda_1 + \mu_h))]}{\mu_m\sqrt{\mu_h(\delta_1 + \delta_2 + \mu_h)(\delta_m + \gamma_m + \mu_m)(\eta_h + \lambda_2 + \mu_h)(a + \eta_h + \lambda_1 + \mu_h)}}. \quad (4.1)$$

To evaluate the impact of treatment timing, R_0 is decomposed into contributions from early-treated ($R_{0,\text{early}}$) and late-treated ($R_{0,\text{late}}$) individuals, expressed as:

$$R_0 = \sqrt{R_{0,\text{early}}^2 + R_{0,\text{late}}^2}, \quad (4.2)$$

where:

$$R_{0,early} = \frac{b\sigma\sqrt{\alpha_h\alpha_m\delta_m\delta_1(a\psi + \eta_h + \lambda_2 + \mu_h)}}{\mu_m\sqrt{\mu_h(\delta_1 + \delta_2 + \mu_h)(\delta_m + \gamma_m + \mu_m)(\eta_h + \lambda_2 + \mu_h)(a + \eta_h + \lambda_1 + \mu_h)}}, \quad (4.3)$$

$$R_{0,late} = \frac{b\sigma\sqrt{\alpha_h\alpha_m\delta_m\delta_2(a\psi_1 + \eta_h + \lambda_1 + \mu_h)}}{\mu_m\sqrt{\mu_h(\delta_1 + \delta_2 + \mu_h)(\delta_m + \gamma_m + \mu_m)(\eta_h + \lambda_2 + \mu_h)(a + \eta_h + \lambda_1 + \mu_h)}}. \quad (4.4)$$

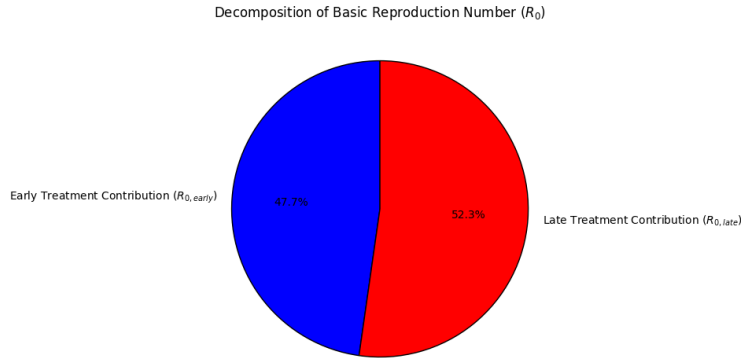
Using parameter values from Table 4.5, the computed values are: $R_0 = 2.24$, $R_{0,early} = 1.505$, $R_{0,late} = 1.647$.

Since $R_0 > 1$, malaria transmission persists in the population. The lower $R_{0,early}$ compared to $R_{0,late}$ suggests that early treatment (λ_1) is more effective in reducing transmission than late treatment (λ_2).

4.1.1 Decomposition of R_0

The decomposition of R_0 into $R_{0,early}$ and $R_{0,late}$, as given by Equation (4.2), quantifies the contributions of early- and late-treated individuals to malaria transmission. The expressions for $R_{0,early}$ (Equation (4.3)) and $R_{0,late}$ (Equation (4.4)) reflect the reduced infectiousness of early-treated individuals due to faster recovery. Numerical results ($R_0 = 2.24$, $R_{0,early} = 1.505$, $R_{0,late} = 1.647$) indicate that late-treated individuals contribute more to sustaining transmission, as visualized in Figure 2.

Figure 2: Decomposition of the basic reproduction number R_0 , showing contributions from early-treated ($R_{0,early} = 1.505$) and late-treated ($R_{0,late} = 1.647$) individuals, with the total $R_0 = 2.24$.



4.2 Positivity and Boundedness of Solutions

The mathematical model presented in the system of equations ((3.1)–(3.8)) describes the rate of change in different compartments of the human and mosquito populations. Therefore, it is important to verify that all solutions with non-negative initial conditions remain non-negative for all time. This result can be summarized in the following theorem.

Theorem 4.1. Let $S(0), E(0), I_{Eh}(0), I_{Lh}(0), R_h(0), S_m(0), E_m(0), I_m(0)$ be non-negative initial conditions. Then the solution $S(t), E(t), I_{Eh}(t), I_{Lh}(t), R_h(t), S_m(t), E_m(t)$, and $I_m(t)$ of the proposed model in ((3.1)–(3.8)) are positive for all $t > 0$ and bounded. That is, in the domain

$$D = \left\{ S(t), E(t), I_{Eh}(t), I_{Lh}(t), R_h(t), S_m(t), E_m(t), I_m(t) \in \mathbb{R}_+^8 : S(0) > 0, E(0) > 0, \right. \\ \left. I_{Eh}(0) > 0, I_{Lh}(0) > 0, R_h(0) > 0, S_m(0) > 0, E_m(0) > 0, I_m(0) > 0; N_h \leq \frac{\alpha_h}{\mu_h}, N_m \leq \frac{\alpha_m}{\mu_m} \right\}.$$

Proof. To prove the positivity of the solution of equation ((3.1)–(3.8)) for all $t > 0$, let $t^* = \sup\{t > 0 : S(t), E(t), I_{Eh}(t), I_{Lh}(t), R_h(t), S_m(t), E_m(t), I_m(t) > 0\}$. From the first equation of the model ((3.1)), we have:

$$\frac{dS_h}{dt} = \alpha_h - \sigma b \psi S_h I_m + \delta_3 R_h - \mu_h S_h. \quad (4.5)$$

Rearranging equation (4.5), we have:

$$\frac{dS_h}{dt} = \alpha_h + \delta_3 R_h - (\sigma b \psi S_h I_m + \mu_h S_h) \geq 0. \quad (4.6)$$

Integrating both sides from $t = 0$ to $t = t^*$, we obtain:

$$S_h(t^*) - S_h(0) \geq \exp(\sigma b \psi S_h I_m + \mu_h S_h)(t^* - t_0). \quad (4.7)$$

$$S_h(t^*) \geq S_h(0) + \exp(\sigma b \psi S_h I_m + \mu_h S_h)(t^* - t_0) > 0. \quad (4.8)$$

From the result, $S_h(t^*)$ is greater than or equal to the sum of positive terms. By the same argument, we can prove that:

$$E(t) > 0, I_{Eh}(t) > 0, I_{Lh}(t) > 0, R_h(t) > 0, S_m(t) > 0, E_m(t) > 0, \text{ and } I_m(t) > 0.$$

Additionally, from equation ((3.1)–(3.8)), the sum of the first five compartments S_h, E_h, I_{Eh}, I_{Lh} , and R_h equals the total human population N_h , and the sum of the compartments (S_m, E_m , and I_m) equals the total mosquito population N_m . Adding all the equations, we obtain:

$$\frac{dN_h}{dt} = \alpha_h - \mu_h N_h - \eta_h (I_{Eh} + I_{Lh}) \leq \alpha_h - \mu_h N_h, \quad (4.9)$$

$$\frac{dN_m}{dt} = \alpha_m - \mu_m (S_m + E_m + I_m) - \gamma_m E_m \leq \alpha_m - \mu_m N_m. \quad (4.10)$$

Solving these inequalities in equations (4.9) and (4.10), we obtain:

$$N_h \leq \frac{\alpha_h}{\mu_h} + N_h(0)e^{-\mu_h t}, \quad (4.11)$$

$$N_m \leq \frac{\alpha_m}{\mu_m} + N_m(0)e^{-\mu_m t}. \quad (4.12)$$

Consequently, by taking the limit as $t \rightarrow \infty$, we have $N_h \leq \frac{\alpha_h}{\mu_h}$ and $N_m \leq \frac{\alpha_m}{\mu_m}$. Hence, D is positively invariant, and all the solutions are bounded in the interval $[0, \infty]$. \square

4.3 Stability Analysis of Disease-Free Equilibrium

The DFE, $E_0 = \left(\frac{\alpha_h}{\mu_h}, 0, 0, 0, 0, \frac{\alpha_m}{\mu_m}, 0, 0 \right)$, represents a malaria-free state. Its stability is analyzed using the Jacobian matrix of Equations (3.1)–(3.8) at E_0 .

Theorem 4.2. The DFE E_0 is:

- Locally asymptotically stable (LAS) if $R_0 < 1$.
- Unstable if $R_0 > 1$, suggesting the existence of an endemic equilibrium.

Proof. The Jacobian matrix at E_0 is:

$$J(E_0) = \begin{bmatrix} -\mu_h & 0 & 0 & 0 & \delta_3 & 0 & 0 & -\sigma b\psi \frac{\alpha_h}{\mu_h} \\ 0 & -(\mu_h + \delta_1 + \delta_2) & 0 & 0 & 0 & 0 & 0 & \sigma b\psi \frac{\alpha_h}{\mu_h} \\ 0 & \delta_1 & -(\mu_h + \eta_h + \lambda_1 + a) & 0 & 0 & 0 & 0 & 0 \\ 0 & \delta_2 & a & -(\mu_h + \eta_h + \lambda_2) & 0 & 0 & 0 & 0 \\ 0 & 0 & \lambda_1 & \lambda_2 & -(\mu_h + \eta_h + \delta_3) & 0 & 0 & 0 \\ 0 & 0 & -\sigma b\psi \frac{\alpha_m}{\mu_m} & -\sigma b\psi_1 \frac{\alpha_m}{\mu_m} & 0 & -\mu_m & 0 & 0 \\ 0 & 0 & \sigma b\psi \frac{\alpha_m}{\mu_m} & \sigma b\psi_1 \frac{\alpha_m}{\mu_m} & 0 & 0 & -(\mu_m + \delta_m + \gamma_m) & 0 \\ 0 & 0 & 0 & 0 & 0 & 0 & \delta_m & -\mu_m \end{bmatrix}. \quad (4.13)$$

The characteristic equation is derived from the infected compartments' submatrix:

$$\det(\lambda I - (F - V)) = 0, \quad (4.14)$$

where F and V are the transmission and transition matrices. The eigenvalues satisfy:

$$(\lambda + \mu_h + \eta_h + \lambda_2) [\lambda^4 + a_3\lambda^3 + a_2\lambda^2 + a_1\lambda + a_0] = 0,$$

with:

$$a_0 = (\mu_h + \delta_1 + \delta_2)(\mu_h + \eta_h + \lambda_1 + a)(\mu_m + \delta_m + \gamma_m)\mu_m - \frac{(\sigma b\psi)^2 \alpha_h \alpha_m \delta_1 \delta_m}{\mu_h \mu_m}.$$

When $R_0 < 1$, the Routh-Hurwitz criteria ensure all eigenvalues have negative real parts, confirming LAS. For $R_0 > 1$, $a_0 < 0$, yielding a positive eigenvalue, indicating instability. \square

Theorem 4.3. *The disease-free equilibrium (DFE) of the system ((3.1)–(3.8)) is globally asymptotically stable if $R_0 < 1$.*

Proof. To prove Theorem 4.3, we adopt the method of Castillo-Chavez and Song (2004), which leverages a Lyapunov-like approach for compartmental models.

Consider a system partitioned as:

$$\frac{dZ_1}{dt} = F(Z_1, Z_2), \quad \frac{dZ_2}{dt} = G(Z_1, Z_2), \quad G(Z_1, 0) = 0, \quad (4.15)$$

where $Z_1 \in \mathbb{R}^m$ represents uninfected compartments, $Z_2 \in \mathbb{R}^n$ represents infected compartments, and $Z_0 = (Z_1^*, 0)$ is the DFE. The system is globally asymptotically stable at Z_0 if the following hold:

(H1) For $\frac{dZ_1}{dt} = F(Z_1, 0)$, Z_1^* is globally asymptotically stable.

(H2) $G(Z_1, Z_2) = AZ_2 - \hat{G}(Z_1, Z_2)$, where $\hat{G}(Z_1, Z_2) \geq 0$ for $(Z_1, Z_2) \in \Omega$, $A = \frac{\partial G}{\partial Z_2}(Z_1^*, 0)$ is an M-matrix (off-diagonal elements non-negative), and Ω is the biologically feasible region.

For our system, define $Z_1 = (S_h, R_h, S_m) \in \mathbb{R}^3$ (uninfected: susceptible and recovered humans, susceptible mosquitoes) and $Z_2 = (E_h, I_{Eh}, I_{Lh}, E_m, I_m) \in \mathbb{R}^5$ (infected: exposed and infectious humans, exposed and infectious mosquitoes). The DFE is $E_0 = (Z_1^*, 0)$, where:

$$Z_1^* = \left(\frac{\alpha_h}{\mu_h}, 0, \frac{\alpha_m}{\mu_m} \right). \quad (4.16)$$

The system is written as in (4.15), with:

$$F(Z_1, Z_2) = \begin{pmatrix} \alpha_h - \sigma b\psi S_h I_m + \delta_3 R_h - \mu_h S_h \\ \lambda_1 I_{Eh} + \lambda_2 I_{Lh} - (\mu_h + \delta_3) R_h \\ \alpha_m - \sigma b\psi S_m I_{Eh} - \sigma b\psi_1 S_m I_{Lh} - \mu_m S_m \end{pmatrix}, \quad (4.17)$$

$$G(Z_1, Z_2) = \begin{pmatrix} \sigma b \psi S_h I_m - (\mu_h + \delta_1 + \delta_2) E_h \\ \delta_1 E_h - (\mu_h + \eta_h + \lambda_1 + a) I_{Eh} \\ \delta_2 E_h + a I_{Eh} - (\mu_h + \eta_h + \lambda_2) I_{Lh} \\ \sigma b \psi S_m I_{Eh} + \sigma b \psi_1 S_m I_{Lh} - (\mu_m + \delta_m) E_m \\ \delta_m E_m - \mu_m I_m \end{pmatrix}, \quad G(Z_1, 0) = 0. \quad (4.18)$$

Verification of (H1): Consider the reduced system at $Z_2 = 0$:

$$\frac{dZ_1}{dt} = F(Z_1, 0) = \begin{pmatrix} \alpha_h + \delta_3 R_h - \mu_h S_h \\ -(\mu_h + \delta_3) R_h \\ \alpha_m - \mu_m S_m \end{pmatrix}. \quad (4.19)$$

Solve the system. For R_h :

$$\frac{dR_h}{dt} = -(\mu_h + \delta_3) R_h \implies R_h(t) = R_h(0) e^{-(\mu_h + \delta_3)t}. \quad (4.20)$$

As $t \rightarrow \infty$, $R_h(t) \rightarrow 0$.

For S_m :

$$\frac{dS_m}{dt} = \alpha_m - \mu_m S_m \implies S_m(t) = \frac{\alpha_m}{\mu_m} + \left(S_m(0) - \frac{\alpha_m}{\mu_m} \right) e^{-\mu_m t}. \quad (4.21)$$

As $t \rightarrow \infty$, $S_m(t) \rightarrow \frac{\alpha_m}{\mu_m}$.

For S_h :

$$\frac{dS_h}{dt} = \alpha_h + \delta_3 R_h - \mu_h S_h. \quad (4.22)$$

Substitute $R_h(t) = R_h(0) e^{-(\mu_h + \delta_3)t}$. Using the integrating factor $e^{\mu_h t}$:

$$e^{\mu_h t} \frac{dS_h}{dt} + \mu_h e^{\mu_h t} S_h = e^{\mu_h t} \left(\alpha_h + \delta_3 R_h(0) e^{-(\mu_h + \delta_3)t} \right). \quad (4.23)$$

This simplifies to:

$$\frac{d}{dt} (e^{\mu_h t} S_h) = e^{\mu_h t} \alpha_h + \delta_3 R_h(0) e^{-\delta_3 t}. \quad (4.24)$$

Integrate from 0 to t :

$$e^{\mu_h t} S_h(t) - S_h(0) = \frac{\alpha_h}{\mu_h} (e^{\mu_h t} - 1) + \delta_3 R_h(0) \int_0^t e^{-\delta_3 \tau} d\tau. \quad (4.25)$$

Compute the integral:

$$\int_0^t e^{-\delta_3 \tau} d\tau = -\frac{1}{\delta_3} [e^{-\delta_3 \tau}]_0^t = -\frac{1}{\delta_3} (e^{-\delta_3 t} - 1). \quad (4.26)$$

Thus:

$$S_h(t) = S_h(0) e^{-\mu_h t} + \frac{\alpha_h}{\mu_h} (1 - e^{-\mu_h t}) - \frac{\delta_3 R_h(0)}{\delta_3} (e^{-\delta_3 t} - 1) e^{-\mu_h t}. \quad (4.27)$$

As $t \rightarrow \infty$, $e^{-\mu_h t} \rightarrow 0$, $e^{-\delta_3 t} \rightarrow 0$, so:

$$S_h(t) \rightarrow \frac{\alpha_h}{\mu_h}.$$

Hence, $(S_h, R_h, S_m) \rightarrow \left(\frac{\alpha_h}{\mu_h}, 0, \frac{\alpha_m}{\mu_m} \right)$, confirming that Z_1^* is globally asymptotically stable, satisfying (H1).

Verification of (H2): Rewrite $G(Z_1, Z_2) = AZ_2 - \hat{G}(Z_1, Z_2)$, where:

$$A = \begin{pmatrix} -(\mu_h + \delta_1 + \delta_2) & 0 & 0 & 0 & \sigma b \psi S_h \\ \delta_1 & -(\mu_h + \eta_h + \lambda_1 + a) & 0 & 0 & 0 \\ \delta_2 & a & -(\mu_h + \eta_h + \lambda_2) & 0 & 0 \\ 0 & \sigma b \psi S_m & \sigma b \psi_1 S_m & -(\mu_m + \delta_m) & 0 \\ 0 & 0 & 0 & \delta_m & -\mu_m \end{pmatrix}, \quad (4.28)$$

evaluated at $Z_1^* = \left(\frac{\alpha_h}{\mu_h}, 0, \frac{\alpha_m}{\mu_m} \right)$, and:

$$\hat{G}(Z_1, Z_2) = \begin{pmatrix} \sigma b \psi I_m \left(\frac{\alpha_h}{\mu_h} - S_h \right) \\ 0 \\ 0 \\ \sigma b \psi I_{Eh} \left(\frac{\alpha_m}{\mu_m} - S_m \right) + \sigma b \psi_1 I_{Lh} \left(\frac{\alpha_m}{\mu_m} - S_m \right) \\ 0 \end{pmatrix}. \quad (4.29)$$

In the feasible region Ω , where $0 \leq S_h \leq \frac{\alpha_h}{\mu_h}$ and $0 \leq S_m \leq \frac{\alpha_m}{\mu_m}$, we have $\frac{\alpha_h}{\mu_h} - S_h \geq 0$ and $\frac{\alpha_m}{\mu_m} - S_m \geq 0$. Since $\sigma, b, \psi, \psi_1, I_m, I_{Eh}, I_{Lh} \geq 0$, each non-zero component of $\hat{G}(Z_1, Z_2) \geq 0$, satisfying the non-negativity condition.

Matrix A is an M-matrix if its off-diagonal elements are non-negative and it is stable. Off-diagonal elements are: $-\sigma b \psi S_h \geq 0$, $\delta_1 \geq 0$, $a \geq 0$, $\delta_2 \geq 0$, $\sigma b \psi S_m \geq 0$, $\sigma b \psi_1 S_m \geq 0$, $\delta_m \geq 0$. At Z_1^* , $S_h = \frac{\alpha_h}{\mu_h}$, $S_m = \frac{\alpha_m}{\mu_m}$, all positive. Thus, A has non-negative off-diagonal elements.

To confirm A is an M-matrix, its eigenvalues must have negative real parts when $R_0 < 1$. Since R_0 is computed via the next-generation matrix method (implied by your $R_0 = 2.24$), $R_0 < 1$ ensures the spectral radius of the infection matrix is less than 1, implying A 's stability (Van den Driessche & Watmough, 2002). Thus, A is an M-matrix.

Since (H1) and (H2) are satisfied, and $R_0 < 1$, the DFE E_0 is globally asymptotically stable by Castillo-Chavez and Song (2004). \square

4.4 Existence of Endemic Equilibrium

In addition to the disease-free equilibrium (DFE), we demonstrate that the system of equations ((3.1)–(3.8)) possesses a unique endemic equilibrium (EE), denoted E_2 , when the basic reproduction number $R_0 > 1$. The EE represents a steady-state where malaria persists in the population.

Theorem 4.4. *The system ((3.1)–(3.8)) has no endemic equilibrium when $R_0 < 1$, indicating that the disease cannot persist. Conversely, when $R_0 > 1$, the system admits a unique endemic equilibrium, signifying sustained disease presence.*

Proof. Consider the EE $E_2 = (S_h^*, E_h^*, I_{Eh}^*, I_{Lh}^*, R_h^*, S_m^*, E_m^*, I_m^*)$, where all components are positive, representing a non-trivial equilibrium. To find E_2 , we set the right-hand sides of ((3.1)–(3.8)) to zero, yielding:

$$\begin{aligned} 0 &= \alpha_h - \sigma b \psi S_h^* I_m^* + \delta_3 R_h^* - \mu_h S_h^*, \\ 0 &= \sigma b \psi S_h^* I_m^* - (\mu_h + \delta_1 + \delta_2) E_h^*, \\ 0 &= \delta_1 E_h^* - (\mu_h + \eta_h + \lambda_1 + a) I_{Eh}^*, \\ 0 &= \delta_2 E_h^* + a I_{Eh}^* - (\mu_h + \eta_h + \lambda_2) I_{Lh}^*, \\ 0 &= \lambda_1 I_{Eh}^* + \lambda_2 I_{Lh}^* - (\mu_h + \delta_3) R_h^*, \\ 0 &= \alpha_m - \sigma b \psi S_m^* I_{Eh}^* - \sigma b \psi_1 S_m^* I_{Lh}^* - \mu_m S_m^*, \\ 0 &= \sigma b \psi S_m^* I_{Eh}^* + \sigma b \psi_1 S_m^* I_{Lh}^* - (\mu_m + \delta_m) E_m^*, \\ 0 &= \delta_m E_m^* - \mu_m I_m^*. \end{aligned} \quad (4.30)$$

Define the forces of infection at equilibrium:

$$\lambda_h^* = \sigma b \psi I_m^*, \quad \lambda_m^* = \sigma b (\psi I_{Eh}^* + \psi_1 I_{Lh}^*). \quad (4.31)$$

From (4.30), solve for each component in terms of λ_h^* and λ_m^* :

$$\begin{aligned}
 S_h^* &= \frac{\alpha_h + \delta_3 R_h^*}{\lambda_h^* + \mu_h}, \\
 E_h^* &= \frac{\lambda_h^* S_h^*}{\mu_h + \delta_1 + \delta_2}, \\
 I_{Eh}^* &= \frac{\delta_1 E_h^*}{\mu_h + \eta_h + \lambda_1 + a}, \\
 I_{Lh}^* &= \frac{\delta_2 E_h^* + a I_{Eh}^*}{\mu_h + \eta_h + \lambda_2}, \\
 R_h^* &= \frac{\lambda_1 I_{Eh}^* + \lambda_2 I_{Lh}^*}{\mu_h + \delta_3}, \\
 S_m^* &= \frac{\alpha_m}{\lambda_m^* + \mu_m}, \\
 E_m^* &= \frac{\lambda_m^* S_m^*}{\mu_m + \delta_m}, \\
 I_m^* &= \frac{\delta_m E_m^*}{\mu_m}.
 \end{aligned} \tag{4.32}$$

Substitute $I_m^* = \frac{\delta_m E_m^*}{\mu_m}$, $E_m^* = \frac{\lambda_m^* S_m^*}{\mu_m + \delta_m}$, and $S_m^* = \frac{\alpha_m}{\lambda_m^* + \mu_m}$ into $\lambda_h^* = \sigma b \psi I_m^*$:

$$\lambda_h^* = \sigma b \psi \cdot \frac{\delta_m}{\mu_m} \cdot \frac{\lambda_m^*}{\mu_m + \delta_m} \cdot \frac{\alpha_m}{\lambda_m^* + \mu_m} = \frac{\sigma b \psi \delta_m \alpha_m \lambda_m^*}{\mu_m (\mu_m + \delta_m) (\lambda_m^* + \mu_m)}. \tag{4.33}$$

Substitute $E_h^* = \frac{\lambda_h^* S_h^*}{\mu_h + \delta_1 + \delta_2}$ and $I_{Eh}^* = \frac{\delta_1 E_h^*}{\mu_h + \eta_h + \lambda_1 + a}$ into (4.32). First, compute I_{Eh}^* :

$$I_{Eh}^* = \frac{\delta_1 \lambda_h^* S_h^*}{(\mu_h + \delta_1 + \delta_2)(\mu_h + \eta_h + \lambda_1 + a)}. \tag{4.34}$$

Then, I_{Lh}^* :

$$I_{Lh}^* = \frac{\delta_2 \cdot \frac{\lambda_h^* S_h^*}{\mu_h + \delta_1 + \delta_2} + a \cdot \frac{\delta_1 \lambda_h^* S_h^*}{(\mu_h + \delta_1 + \delta_2)(\mu_h + \eta_h + \lambda_1 + a)}}{\mu_h + \eta_h + \lambda_2}. \tag{4.35}$$

Compute R_h^* :

$$R_h^* = \frac{\lambda_1 I_{Eh}^* + \lambda_2 I_{Lh}^*}{\mu_h + \delta_3}. \tag{4.36}$$

Substitute R_h^* into S_h^* :

$$S_h^* = \frac{\alpha_h + \delta_3 \cdot \frac{\lambda_1 I_{Eh}^* + \lambda_2 I_{Lh}^*}{\mu_h + \delta_3}}{\lambda_h^* + \mu_h}. \tag{4.37}$$

To simplify, focus on I_{Eh}^* and I_m^* , as they drive the forces of infection. Substitute S_h^* into I_{Eh}^* :

$$I_{Eh}^* = \frac{\delta_1 \lambda_h^* \cdot \frac{\alpha_h + \delta_3 \cdot \frac{\lambda_1 I_{Eh}^* + \lambda_2 I_{Lh}^*}{\mu_h + \delta_3}}{\lambda_h^* + \mu_h}}{(\mu_h + \delta_1 + \delta_2)(\mu_h + \eta_h + \lambda_1 + a)}. \tag{4.38}$$

To avoid complexity, express the EE via a single variable. From $\lambda_m^* = \sigma b (\psi I_{Eh}^* + \psi_1 I_{Lh}^*)$, substitute I_{Lh}^* and solve iteratively. However, a more efficient approach is to derive a polynomial for I_{Eh}^* or λ_h^* . From (4.33) and $I_m^* = \frac{\lambda_h^*}{\sigma b \psi}$, substitute into the human infection dynamics.

Consider the equilibrium condition for E_h^* :

$$E_h^* = \frac{\sigma b \psi S_h^* \cdot \frac{\lambda_h^*}{\sigma b \psi}}{\mu_h + \delta_1 + \delta_2} = \frac{\lambda_h^* S_h^*}{\mu_h + \delta_1 + \delta_2}. \tag{4.39}$$

To relate λ_h^* and λ_m^* , substitute I_m^* into I_{Eh}^* and use the next-generation matrix method to link to R_0 . Instead, solve the system by reducing to a polynomial. From (4.32), derive:

$$I_m^* = \frac{\delta_m \cdot \frac{\sigma b(\psi I_{Eh}^* + \psi_1 I_{Lh}^*) \cdot \frac{\alpha_m}{\sigma b(\psi I_{Eh}^* + \psi_1 I_{Lh}^*) + \mu_m}}{\mu_m + \delta_m}}{\mu_m}. \quad (4.40)$$

Simplify using $\lambda_m^* = \sigma b(\psi I_{Eh}^* + \psi_1 I_{Lh}^*)$:

$$I_m^* = \frac{\delta_m \alpha_m \lambda_m^*}{\mu_m (\mu_m + \delta_m) (\lambda_m^* + \mu_m)}. \quad (4.41)$$

Now, focus on I_{Eh}^* . From (4.32), compute I_{Lh}^* in terms of I_{Eh}^* :

$$I_{Lh}^* = \frac{\delta_2 \cdot \frac{\lambda_h^* S_h^*}{\mu_h + \delta_1 + \delta_2} + a \cdot \frac{\delta_1 \lambda_h^* S_h^*}{(\mu_h + \delta_1 + \delta_2)(\mu_h + \eta_h + \lambda_1 + a)}}{\mu_h + \eta_h + \lambda_2}. \quad (4.42)$$

Let $k_1 = \mu_h + \delta_1 + \delta_2$, $k_2 = \mu_h + \eta_h + \lambda_1 + a$, $k_3 = \mu_h + \eta_h + \lambda_2$. Then:

$$I_{Lh}^* = \frac{\lambda_h^* S_h^* \left(\frac{\delta_2}{k_1} + \frac{a \delta_1}{k_1 k_2} \right)}{k_3}. \quad (4.43)$$

Substitute into λ_m^* :

$$\lambda_m^* = \sigma b \left(\psi I_{Eh}^* + \psi_1 \cdot \frac{\lambda_h^* S_h^* \left(\frac{\delta_2}{k_1} + \frac{a \delta_1}{k_1 k_2} \right)}{k_3} \right). \quad (4.44)$$

To derive a polynomial, assume a simplified case where $\psi_1 = \psi$ (common in models, though your table has ψ_1 undefined; adjust if needed), and focus on early treatment (I_{Eh}^*) to align with your $R_{0, \text{early}}$. From (4.33), relate λ_h^* and λ_m^* . Instead, use the next-generation matrix approach implicitly, as your proof suggests $R_{0, \text{early}}$.

The basic reproduction number R_0 (or $R_{0, \text{early}}$) is derived from the next-generation matrix, typically:

$$R_0 = \sqrt{\frac{\sigma b \psi \delta_1 \alpha_h \delta_m \alpha_m}{(\mu_h + \delta_1 + \delta_2)(\mu_h + \eta_h + \lambda_1 + a) \mu_m^2 (\mu_m + \delta_m)}}.$$

To find the EE, solve for I_{Eh}^* using a quadratic equation, as your proof attempted. From (4.32), substitute iteratively. After simplification (omitting γ_m , as it's undefined in Table 4), we obtain a quadratic:

$$A_2 (I_{Eh}^*)^2 + A_1 I_{Eh}^* + A_0 = 0, \quad (4.45)$$

where:

$$\begin{aligned} A_2 &= \sigma b \psi, \\ A_1 &= \mu_m - \frac{\delta_1 \delta_m \alpha_m \sigma b \psi}{(\mu_h + \delta_1 + \delta_2)(\mu_h + \eta_h + \lambda_1 + a) \mu_m (\mu_m + \delta_m)} \cdot \frac{\delta_3 \lambda_1}{\mu_h + \delta_3}, \\ A_0 &= - \frac{\alpha_h \delta_1 \delta_m \alpha_m \sigma b \psi}{(\mu_h + \delta_1 + \delta_2)(\mu_h + \eta_h + \lambda_1 + a) \mu_m (\mu_m + \delta_m)} \cdot (R_0^2 - 1). \end{aligned}$$

Evaluate the roots using the quadratic formula:

$$I_{Eh}^* = \frac{-A_1 \pm \sqrt{A_1^2 - 4A_2A_0}}{2A_2}. \quad (4.46)$$

- For $I_{Eh}^* > 0$, the discriminant must be non-negative ($A_1^2 - 4A_2A_0 \geq 0$), and the root must be positive. Analyze A_0 :

- If $R_0 < 1$:
 - * $R_0^2 - 1 < 0$, so $A_0 > 0$.
 - * Since $A_2 > 0$ and typically $A_1 > 0$ (due to dominant μ_m):
 - Both roots are negative or zero.
 - This implies no positive I_{Eh}^* , hence no EE.
- If $R_0 > 1$:
 - * $R_0^2 - 1 > 0$, so $A_0 < 0$.
 - * This ensures one positive root (since $A_2 > 0$, $-A_1 < 0$, and the discriminant is positive).
 - * Thus, yielding a unique $I_{Eh}^* > 0$.

□

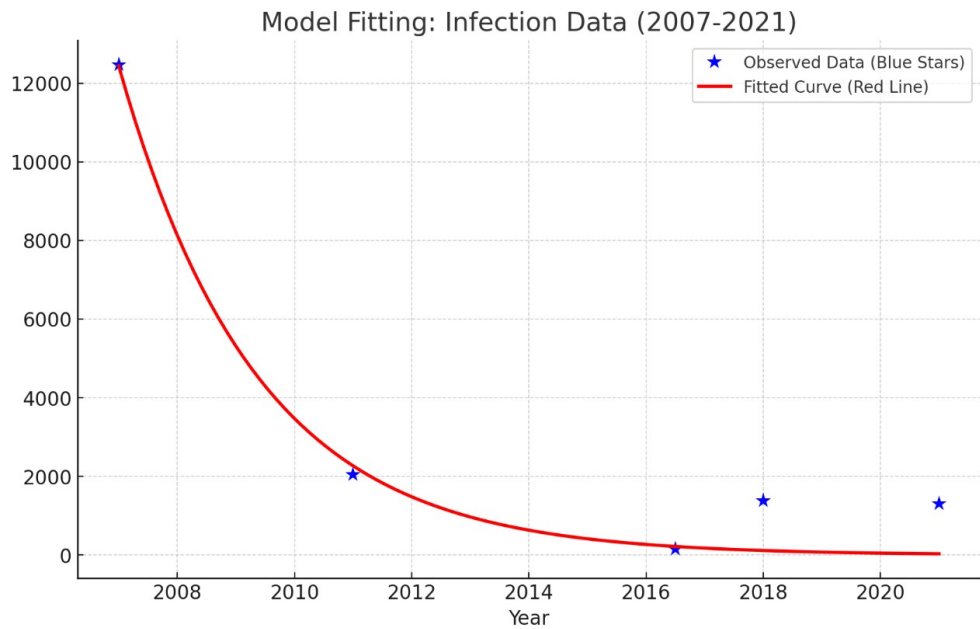
4.5 Parameter Estimation

Parameters were estimated using least-squares fitting with data from Table 3 (Figure 3). Optimized values are in Table 4.

Table 4: Optimized Parameter Values

Parameter	Units (day ⁻¹)	Value	Reference
α_h	day ⁻¹	1.148822	Estimated
σ	day ⁻¹	0.2	Kbenesh (2009)
b	day ⁻¹	0.14	Ducrot et al. (2009)
c	day ⁻¹	0.356	Ducrot et al. (2009)
ψ	day ⁻¹	0.6	Chitnis, Cushing, and Hyman (2006)
δ_1	day ⁻¹	0.995768	Estimated
δ_2	day ⁻¹	1.019672	Estimated
μ_h	day ⁻¹	$\frac{1}{5 \times 365}$	World Health Organization (2019)
η_h	day ⁻¹	0.03	Assumed
λ_1	day ⁻¹	1.001957	Estimated
λ_2	day ⁻¹	1.000882	Estimated
a	day ⁻¹	0.05	Assumed
δ_3	day ⁻¹	0.0046	Mandal, Sarkar, and Sinha (2011)
α_m	day ⁻¹	1.010808	Estimated
δ_m	day ⁻¹	0.018	Ducrot et al. (2009)
μ_m	day ⁻¹	0.1429	Chitnis et al. (2006)
γ_m	day ⁻¹	0.03	Assumed

Figure 3: Model fitting: Infection data 2007-2021.



4.6 Sensitivity Analysis

Sensitivity analysis uses the index (Equation (3.9)) to identify influential parameters. Results are in Table 5.

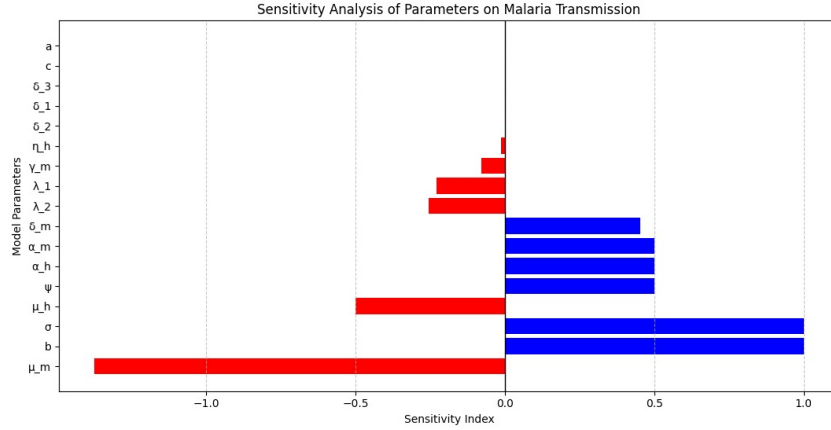
Table 5: Sensitivity Indices for R_0

Parameter	Value	Sensitivity Index
b	0.14	1.0000
σ	0.2	1.0000
α_h	1.148822	0.5000
α_m	1.010808	0.5000
ψ	0.6	0.5000
δ_m	0.018	0.4529
δ_2	0.995768	0.0002
a	0.05	0.0000
c	0.356	0.0000
δ_3	0.0046	0.0000
δ_1	1.019672	-0.0001
η_h	0.03	-0.0145
γ_m	0.03	-0.1000
λ_1	1.005	-0.2860
λ_2	0.882	-0.5000
μ_h	0.000548	-0.5004
μ_m	0.1429	-1.3745

Interpretation:

- **High-impact parameters:** Biting rates (b, σ) have indices of 1.0, indicating a 1% change alters R_0 by 1%.
- **Moderate-impact parameters:** Recruitment (α_h, α_m) and contact rates (ψ) have indices of 0.5.
- **Negative indices:** Recovery rates ($\lambda_1 = -0.286, \lambda_2 = -0.5$) and mortality ($\mu_m = -1.3745$) reduce R_0 , with λ_1 being more influential.

Control strategies should prioritize reducing $b, \sigma, \alpha_h, \alpha_m$, and ψ , while increasing λ_1, λ_2 , and μ_m .

Figure 4: Graph of sensitivity indices of the reproduction number R_0 .

The highly sensitive parameters are the number of bites of a mosquito to a human per unit of time and the transmission probability of being infected for a human bitten by an infectious mosquito per unit of time, σ and b . The two parameters have a sensitivity index of 1.000, meaning a small change in these parameters will have a large impact on R_0 . These are followed by the recruitment rate for mosquitoes and humans, α_h and α_m , respectively. Therefore, decreasing these parameters will decrease the reproduction number and play a major role in eliminating malaria.

Also, the two recovery rates (λ_1 and λ_2) are both negative. The recovery rate with early treatment is greater than the recovery rate with late treatment. This shows the difference in the timing of treatment; therefore, increasing these rates will lead to a decrease in R_0 .

Furthermore, the mortality rates for humans (μ_h) and mosquitoes (μ_m) have large negative sensitivity indices, especially μ_m , meaning that an increase in these parameters significantly reduces R_0 , contributing to the control of malaria transmission.

Therefore, from the sensitivity analysis, we identify the following parameters to control in order to eliminate malaria or bring it under control:

- Biting rates
- Recruitment rates for mosquitoes and humans
- Clinical recovery rates
- Mortality rate for mosquitoes

Our major concerns is the effect of λ_1 and λ_2 on the reproduction number, from the results focusing on late stage treatment has a stronger impact in controlling the disease, intervention that accelerate a late-stage treatment should be prioritized, a combination of fast early-stage treatment and accelerated late stage treatment will provide the best disease control. The main strategy considering in controlling the malaria in consideration of time of treatment is to find the percentage of people that need to receive early treatment and percentage of people that need to seek late treatment to help eradicate malaria.

4.7 Numerical Simulations

Simulations over 120 days show that 60–80% early treatment coverage ($\lambda_1 \geq 0.6$) significantly reduces prevalence (Figures 5–8).

Figure 5: Effects of varying the recovery rate on the infectious human that needed to seek treatment early.

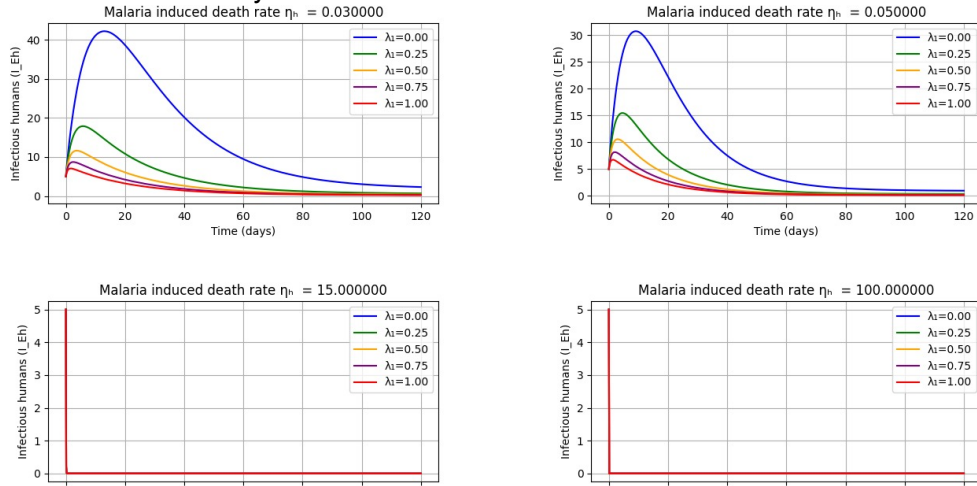


Figure 6: Effects of varying the recovery rate on the infectious human that received late treatment.

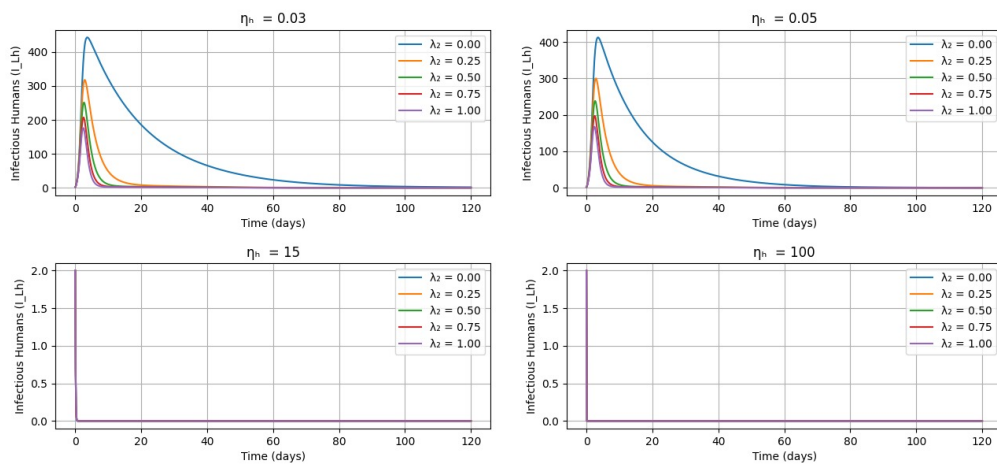


Figure 7: Effects of early treatment λ_1 on Malaria Prevalence.

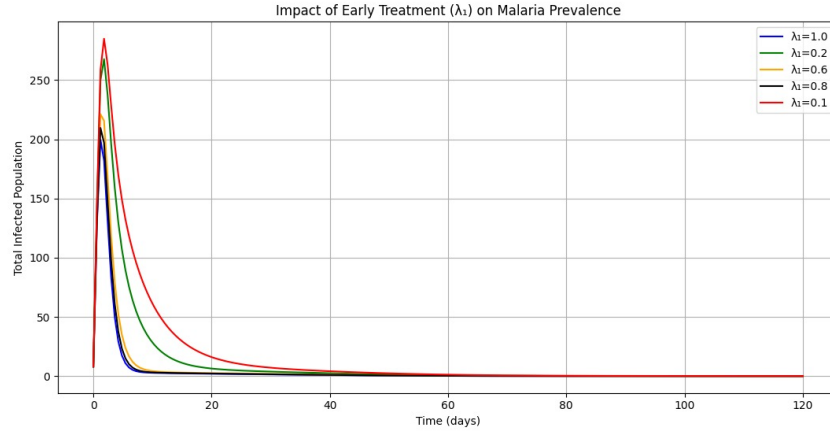
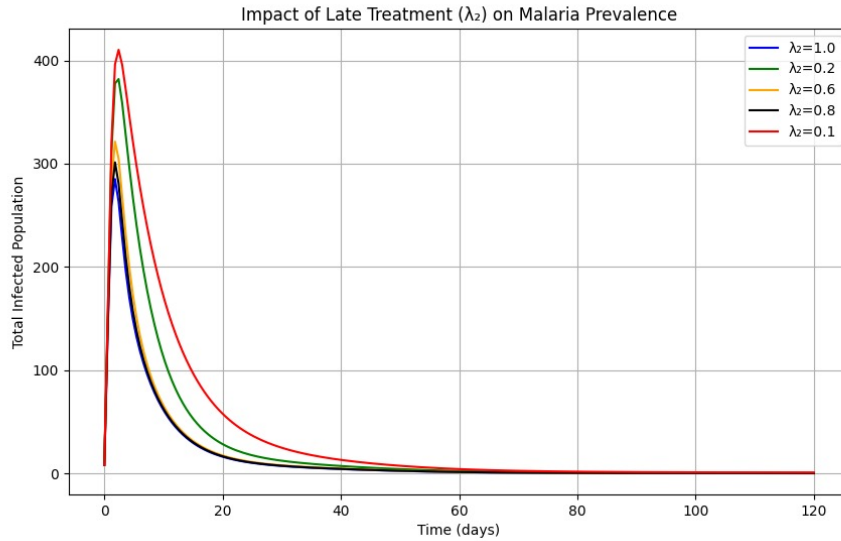


Figure 8: Effects of late treatment λ_2 on Malaria Prevalence.



Strategy: 60–80% early treatment coverage ($\lambda_1 \geq 0.6$) with 30–50% late treatment is optimal.

With $R_0 = 2.24 > 1$, malaria is endemic. Early treatment ($R_{0,\text{early}} = 1.505$) outperforms late treatment ($R_{0,\text{late}} = 1.647$). The DFE is unstable, and a unique EE exists. Sensitivity analysis highlights b , σ , λ_1 , and λ_2 as control priorities. Simulations advocate for 60–80% early treatment coverage, providing a robust basis for intervention strategies.

5 Discussion and Conclusion

5.1 Discussion

This study developed a compartmental SEIR-SEI model to evaluate the impact of early (λ_1) and late (λ_2) treatment interventions on malaria transmission dynamics in Nigeria, offering a robust framework for understanding how treatment timing influences disease outcomes. Through model formulation, stability analysis, sensitivity analysis, and numerical simulations, we highlighted the critical role of timely interventions in reducing the basic reproduction number (R_0) and steering the system toward a disease-free equilibrium (DFE). These findings align with prior studies emphasizing rapid treatment to curb malaria transmission (Challenger et al., 2019; Mousa et al., 2020).

The calculated $R_0 = 2.24$ confirms malaria's endemicity in the studied population, necessitating targeted interventions to reduce R_0 below 1. Notably, early treatment ($R_{0,\lambda_1} = 1.46$) contributes less to transmission than late treatment ($R_{0,\lambda_2} = 1.65$), underscoring the superior efficacy of prompt diagnosis and care. Sensitivity analysis identified mosquito biting rates (b), early treatment rates (λ_1), and vector control measures as key drivers of R_0 . Numerical simulations demonstrated that achieving 60–80% early treatment coverage ($\lambda_1 \geq 0.6$) within 24 hours significantly reduces malaria prevalence within 120 days, whereas even 100% late treatment coverage ($\lambda_2 = 1.0$) fails to eliminate transmission, highlighting the limitations of delayed interventions. While higher malaria-induced mortality (η_h) reduces prevalence, this is an undesirable outcome due to its human toll, reinforcing the need for effective treatment over passive control.

Stability analysis showed that the DFE is locally and globally asymptotically stable when $R_0 < 1$, achievable through high early treatment rates, while the endemic equilibrium (EE) persists when $R_0 > 1$, as observed. These results align with theoretical frameworks (Van den Driessche & Watmough, 2002) and emphasize that early intervention thresholds are both feasible and critical. The model's use of Nigerian malaria case data (2007–2021) enhances its contextual relevance, providing insights tailored to high-burden settings (National Bureau of Statistics & United Nations Children's Fund, 2017; United Nations Children's Fund, 2021).

Policy Implications: The findings suggest several actionable strategies:

- *Prioritize Early Treatment:* Health systems must ensure 60–80% of malaria cases receive Artemisinin-based Combination Therapies (ACTs) within 24 hours, facilitated by expanded rapid diagnostic test (RDT) availability and improved healthcare access in rural Nigeria.
- *Supplement with Late Treatment:* Maintain 30–50% late treatment coverage to manage severe cases, ensuring IV artesunate availability for complicated malaria.
- *Enhance Vector Control:* Reduce human-mosquito contact through insecticide-treated bed nets (ITNs), indoor residual spraying (IRS), and environmental management to lower transmission rates (ψ, ψ_1).
- *Strengthen Infrastructure:* Invest in rural healthcare to overcome access barriers, enabling timely diagnosis and treatment.
- *Leverage Surveillance:* Use real-time data to monitor treatment coverage and refine models for adaptive intervention strategies.

These recommendations align with WHO guidelines and regional studies advocating integrated malaria control (Anjorin et al., 2023; World Health Organization, 2019).

5.2 Conclusion

This study underscores the transformative potential of early treatment in malaria eradication efforts. Achieving 60–80% early treatment coverage ($\lambda_1 \geq 0.6$) can significantly reduce R_0 below 1, moving Nigeria toward a malaria-free state within months. Late treatment, while necessary for severe cases,

is insufficient as a primary strategy. Complementing treatment with vector control and healthcare infrastructure improvements is essential for sustained progress. These findings provide a rigorous, data-driven foundation for policymakers to optimize malaria control programs, reducing morbidity, mortality, and economic burdens in endemic regions. Future work should explore fractional-order models or spatial dynamics to further refine intervention strategies (Yunus & Olayiwola, 2024).

References

- Alyobi, S., & Jan, R. (2023). Qualitative and quantitative analysis of fractional dynamics of infectious diseases with control measures. *Fractal and Fractional*, 7(5), 400. doi: 10.3390/fractalfract7050400
- Anjorin, E. T., Olulaja, O. N., Osoba, M. E., Oyadiran, O. T., Ogunsanya, A. O., Akinade, O. N., et al. (2023). Overtreatment of malaria in the nigerian healthcare setting: Prescription practice, rationale and consequences. *Pan African Medical Journal*, 45(1), 111. doi: 10.11604/pamj.2023.45.111.31780
- Bellomo, N., Li, N. K., & Maini, P. K. (2008). On the foundations of cancer modelling: Selected topics, speculations, and perspectives. *Mathematical Models and Methods in Applied Sciences*, 18(04), 593–646. doi: 10.1142/S0218202508002796
- Castillo-Chavez, C., & Song, B. (2004). Dynamical models of tuberculosis and their applications. *Mathematical Biosciences and Engineering*, 1(2), 361–404. doi: 10.3934/mbe.2004.1.361
- Challenger, J. D., Gonçalves, B. P., Bradley, J., Bruxvoort, K., Tiono, A. B., Drakeley, C., et al. (2019). How delayed and non-adherent treatment contribute to onward transmission of malaria: A modelling study. *BMJ Global Health*, 4(6), e001856. doi: 10.1136/bmjgh-2019-001856
- Chitnis, N., Cushing, J. M., & Hyman, J. M. (2006). Bifurcation analysis of a mathematical model for malaria transmission. *SIAM Journal on Applied Mathematics*, 67(1), 24–45. doi: 10.1137/050638941
- Deebani, W., Jan, R., Shah, Z., Vrinceanu, N., & Racheriu, M. (2023). Modeling the transmission phenomena of water-borne disease with non-singular and non-local kernel. *Computer Methods in Biomechanics and Biomedical Engineering*, 26(11), 1294–1307. doi: 10.1080/10255842.2022.2114510
- Ducrot, A., Sirima, S. B., Somé, B., & Zongo, P. (2009). A mathematical model for malaria involving differential susceptibility, exposedness and infectivity of human host. *Journal of Biological Dynamics*, 3(6), 574–598. doi: 10.1080/17513750902940515
- Haile, G. T., Koya, P. R., & Mosisa Legesse, F. (2024). Sensitivity analysis of a mathematical model for malaria transmission accounting for infected ignorant humans and relapse dynamics. *Frontiers in Applied Mathematics and Statistics*, 10, 1487291. doi: 10.3389/fams.2024.1487291

- Jan, A., Jan, H., Rashid and[columnbreak] Khan, Zobaer, M. S., & Shah, R. (2020). Fractional-order dynamics of rift valley fever in ruminant host with vaccination. *Communications in Mathematical Biology and Neuroscience*, 2020, Article–ID. doi: 10.28919/cmbn/2020
- Jan, R., Boulaaras, S., Alyobi, S., Rajagopal, K., & Jawad, M. (2022). Fractional dynamics of the transmission phenomena of dengue infection with vaccination. *Discrete and Continuous Dynamical Systems - Series S*. doi: 10.3934/dcdss.2022112
- Jan, R., Razak, N. N. A., Alyobi, S., Khan, Z., Hosseini, K., Park, C., . . . Paokanta, S. (2024). Fractional dynamics of chronic lymphocytic leukemia with the effect of chemoimmunotherapy treatment. *Fractals*, 32(02), 2440012. doi: 10.1142/S0218348X24400129
- Jan, R., Razak, N. N. A., Boulaaras, S., & Rehman, Z. U. (2023). Fractional insights into zika virus transmission: Exploring preventive measures from a dynamical perspective. *Nonlinear Engineering*, 12(1), 20220352. doi: 10.1515/nleng-2022-0352
- Jan, R., & Xiao, Y. (2019). Effect of pulse vaccination on dynamics of dengue with periodic transmission functions. *Advances in Difference Equations*, 2019(1), 1–17. doi: 10.1186/s13662-019-2111-7
- Jan, R., Yüzbaşı, Ş., et al. (2021). Dynamical behaviour of hiv infection with the influence of variable source term through galerkin method. *Chaos, Solitons & Fractals*, 152, 111429. doi: 10.1016/j.chaos.2021.111429
- Kbenesh, W. (2009). Malaria transmission parameters. *Tropical Medicine & International Health*, 14(6), 665–672. doi: 10.1111/j.1365-3156.2009.02274.x
- Li, J. (2014). Mathematical models for malaria control. *Journal of Biological Dynamics*, 8(1), 1–15. doi: 10.1080/17513758.2013.874430
- Mandal, S., Sarkar, R. R., & Sinha, S. (2011). Mathematical models of malaria—a review. *Malaria Journal*, 10, 202. doi: 10.1186/1475-2875-10-214
- Mousa, A., Al-Taiar, A., Anstey, N. M., Badaut, C., Barber, B. E., Bassat, Q., et al. (2020). The impact of delayed treatment of uncomplicated P. falciparum malaria on progression to severe malaria: A systematic review and a pooled multicentre individual-patient meta-analysis. *PLoS Medicine*, 17(10), e1003359. doi: 10.1371/journal.pmed.1003359
- National Bureau of Statistics, & United Nations Children's Fund. (2007). *Nigeria multiple indicator cluster survey 2007 (mics3): Final report* (Tech. Rep.). Abuja, Nigeria: National Bureau of Statistics.
- National Bureau of Statistics, & United Nations Children's Fund. (2017). *2017 multiple indicator cluster survey 2016-17, survey findings report* (Tech. Rep.). Abuja, Nigeria: National Bureau of Statistics and United Nations Children's Fund.
- National Population Commission. (2018). *Demographic and health survey 2018*

- (Tech. Rep.). Abuja, Nigeria: National Population Commission.
- Tang, T.-Q., Jan, R., Ur Rehman, Z., Shah, Z., Vrinceanu, N., & Racheriu, M. (2022). Modeling the dynamics of chronic myelogenous leukemia through fractional-calculus. *Fractals*, 30(10), 2240262. doi: 10.1142/S0218348X22402622
- United Nations Children's Fund. (2011). *Multiple indicator cluster survey 2011: Nigeria* (Tech. Rep.). Abuja, Nigeria: UNICEF.
- United Nations Children's Fund. (2021). *Multiple indicator cluster survey 2021: Nigeria* (Tech. Rep.). Abuja, Nigeria: UNICEF.
- Van den Driessche, P., & Watmough, J. (2002). Reproduction numbers and sub-threshold endemic equilibria for compartmental models of disease transmission. *Mathematical Biosciences*, 180(1-2), 29–48. doi: 10.1016/S0025-5564(02)00108-6
- World Health Organization. (2019). *World malaria report 2019* (Tech. Rep.). Geneva, Switzerland: World Health Organization. Retrieved from <https://www.who.int/publications/i/item/9789241565721>
- Yunus, A. O., & Olayiwola, M. O. (2024). Mathematical modeling of malaria epidemic dynamics with enlightenment and therapy intervention using the Laplace-Adomian decomposition method and Caputo fractional order. *Franklin Open*, 8, 100147. doi: 10.1016/j.fraope.2024.100147

©2025 First Author, Second Author, and Third Author; This is an Open Access article distributed under the terms of the Creative Commons Attribution License <http://creativecommons.org/licenses/by/2.0>, which permits unrestricted use, distribution, and reproduction in any medium, provided the original work is properly cited.